Human Cancer Biology

Clinical Cancer Research

Functional Genetic Screens Identify Genes Essential for Tumor Cell Survival in Head and Neck and Lung Cancer

Sanne R. Martens-de Kemp[1], Remco Nagel[1], Marijke Stigter-van Walsum[1], Ida H. van der Meulen[2], Victor W. van Beusechem[2], Boudewijn J.M. Braakhuis[1], and Ruud H. Brakenhoff[1]

Abstract

Purpose: Despite continuous improvement of treatment regimes, the mortality rates for non–small cell lung cancer (NSCLC) and head and neck squamous cell carcinoma (HNSCC) remain disappointingly high and novel anticancer agents are urgently awaited.

Experimental Design: We combined the data from genome-wide siRNA screens on tumor cell lethality in a lung and a head and neck cancer cell line.

Results: We identified 71 target genes that seem essential for the survival of both cancer types. We identified a cluster of 20 genes that play an important role during G_2–M phase transition, underlining the importance of this cell-cycle checkpoint for tumor cell survival. Five genes from this cluster (*CKAP5*, *KPNB1*, *RAN*, *TPX2*, and *KIF11*) were evaluated in more detail and have been shown to be essential for tumor cell survival in both tumor types, but most particularly in HNSCC. Phenotypes that were observed following siRNA-mediated knockdown of *KIF11* (kinesin family member 11) were reproduced by inhibition of KIF11 using the small-molecule inhibitor ispinesib (SB-715992). We showed that ispinesib induces a G_2 arrest, causes aberrant chromosome segregation, and induces cell death in HNSCC *in vitro*, whereas primary keratinocytes are less sensitive. Furthermore, growth of HNSCC cells engrafted in immunodeficient mice was significantly inhibited after ispinesib treatment.

Conclusion: This study identified a wide array of druggable genes for both lung and head and neck cancer. In particular, multiple genes involved in the G_2–M checkpoint were shown to be essential for tumor cell survival, indicating their potential as anticancer targets. *Clin Cancer Res; 19(8); 1994–2003. ©2013 AACR.*

Introduction

Two of the more frequently diagnosed types of cancer in the world are those in the lung and the head and neck region. Lung cancer is currently the most common cancer in the world, whereas head and neck cancer is the sixth most common cancer worldwide (1, 2). The predominant histologic type of head and neck cancer is squamous cell carcinoma (HNSCC), which is found in more than 95% of the cases (3). Lung cancer is more diverse, as multiple different histologic types of tumor cells can be distinguished. Lung cancers are classified as non–small cell lung cancer (NSCLC) and small cell lung cancer (SCLC), which make up approximately 80% and 20% of the total number of cases, respectively (4). NSCLC can be further subdivided into several histologic subtypes, of which squamous cell carcinomas (40%) and adenocarcinomas (37%) are the most predominant (4).

Advanced stages of lung and head and neck cancer are often treated by a combination of platinum-containing chemotherapy and locoregional radiotherapy. Despite improvement of locoregional control, the current survival rates of patients with both lung and head and neck cancer remain disappointing. For HNSCC, the 5-year survival rate is approximately 50% to 60% and this has only increased slightly during the last 3 decades (5). For lung cancer, the prognosis is even worse with a 5-year survival rate of only 5% to 15% (6). Hence, there is an urgent need to improve current therapies. The recent successes with targeted drugs indicate that identification of druggable genes that are essential for tumor cells may fuel the development of novel treatment approaches (7–9).

To survive and proliferate, tumor cells strongly depend on specific genetic and epigenetic alterations. These tumorigenic alterations are responsible for important cancer-associated phenotypes, such as deregulation of apoptosis and cell-cycle control (10). Because these genetic changes drive tumorigenesis, they often become the Achilles' heel of the

Authors' Affiliations: [1]Department of Otolaryngology/Head-Neck Surgery, [2]RNA Interference Functional Oncogenomics Laboratory, Department of Medical Oncology, VU University Medical Center, Amsterdam, the Netherlands

Note: Supplementary data for this article are available at Clinical Cancer Research Online (http://clincancerres.aacrjournals.org/).

S.R. Martens-de Kemp and R. Nagel contributed equally to this work.

Corresponding Author: Ruud H. Brakenhoff, Tumor Biology Section, Department of Otolaryngology/Head-Neck Surgery, VU University Medical Centre, PO Box 7057, 1007 MB Amsterdam. Phone: 31-20-4440953; Fax: 31-20-4443688; E-mail: rh.brakenhoff@vumc.nl

doi: 10.1158/1078-0432.CCR-12-2539

Translational Relevance

The prognosis of lung and head and neck cancer is still disappointing and novel treatments are urgently awaited. In this study, we used a genome-wide siRNA screen to identify genes that seem to be essential for tumor cell viability. A specific subgroup of these genes was linked to G_2–M regulation of the cell cycle and was tested for their suitability as targets to eradicate lung and head and neck cancer cells. A drug against one of these genes, *KIF11*, was tested in xenograft mouse models and inhibited tumor growth significantly. In summary, we show that genome-wide siRNA screens deliver a multitude of druggable genes that can be exploited to improve treatment of both lung and head and neck cancer.

tumor. Moreover, the rewiring of signaling pathways by alterations in the participating genes may cause that expression of some genes becomes very critical for tumor cell survival. Several studies have already reported decreased tumor cell survival by inhibition of individual genes in a specific background of somatic mutations, a phenomenon commonly referred to as synthetic lethality (11–13). Therefore, the identification of genes essential for cell viability and the unmasking of synthetic lethal interactions in tumor cells provide a powerful approach for the discovery of novel therapeutic targets.

Large-scale RNA interference (RNAi) screens are excellently suited for the discovery of genes essential for tumor cell survival. Therefore, in this study, we explored genome-wide siRNA screen data and identified a total of 362 tumor lethal siRNAs. Strikingly, many of the potential tumor essential genes targeted by these siRNAs are involved in the regulation of the G_2–M phase of the cell cycle. Several of these candidates were validated as potent anticancer targets.

Materials and Methods

Cell lines and animal models

The cancer cell lines and primary fibroblasts were cultured in Dulbecco's Modified Eagle's Medium (Lonza), 5% fetal calf serum (Lonza), and 2 mmol/L L-glutamine (Lonza). Oral keratinocytes were cultured in keratinocyte serum-free medium (Invitrogen) supplemented with 0.1% bovine serum albumin (BSA), 25 mg bovine pituitary extract, 2.5 μg human recombinant EGF, 250 μg Amphotericin B (MP biomedicals), and 250 μg gentamycin (Sigma-Aldrich). Cells were grown in a humidified atmosphere of 5% CO_2 at 37°C.

NSCLC cell lines SW1573, A549, H460, and H1299 were obtained from the American Type Culture Collection. HNSCC cell lines UM-SCC-11B, UM-SCC-22A, and UM-SCC-22B were obtained from Dr. T Carey (University of Michigan, Ann Arbor, MI; ref. 14). Cell line VU-SCC-120 (formerly known as 93VU120) and VU-SCC-OE were established as described previously (15). The HNSCC cell lines were authenticated to the earliest available passages by microsatellite profiling and *TP53* mutation analysis (14, 16). Oral keratinocytes and human fibroblasts were isolated from an uvulopalatopharyngoplasty specimen and served as normal control. Use of residual tissue from surgical specimen was according to the guidelines of the Dutch Medical Scientific Societies (www.federa.org) and the Dutch law on medical research. Informed consent was obtained of enrolled patients, when required.

siRNA screens

The SW1573 NSCLC cell line was subjected to a high-throughput forward transfection in 96-well plates (Cellstar, Greiner Bio-One). Cells were seeded using a μFill microplate dispenser (Bio-Tek) and 24 hours later, the cells were transfected on an automated platform. In total 25 nmol of each siRNA SMARTpool derived from the siARRAY Human Genome library [Catalog items G-003500 (Sept05), G-003600 (Sept05), G-004600 (Sept05) and G-005000 (Oct05); Dharmacon, Thermo Fisher Scientific) and 0.01 μL DharmaFECT1 (Thermo Fisher Scientific) were delivered to the cells using the Sciclone ALH 3000 workstation (Caliper LifeSciences) and a Twister II microplate handler (Caliper LifeSciences). The nontargeting siCONTROL#2 and the PLK1 SMARTpool were used as negative and positive control, respectively. Plates were incubated for 96 hours at 37°C/5% CO_2. Afterwards, the cells were fixed and stained for 1 hour with a 3.7% formaldehyde solution in H_2O containing 0.5 μg/mL Hoechst 33342. The number of cells was determined using the Acumen eX3 microplate cytometer (TTP LabTech) by automatically counting the number of nuclei present in each well.

VU-SCC-120 cells were plated and transfected in 96-well flat-bottom low evaporation TPP plates (VWR International) using the aforementioned automated platform and assay controls. Cells were transfected with 25 nmol siRNA and 0.03 μL DharmaFECT1. Cell viability was determined by adding CellTiter-Blue Reagent (Promega) using a Multidrop Combi (Thermo Fisher Scientific) in cell culture medium. After 2 hours of incubation at 37°C, fluorescence was analyzed at 540 nm excitation and 590 nm emission wavelength using an Infinite F200 microplate reader (Tecan).

Deconvolution of cancer-lethal siRNA pools

To validate the potency of the obtained hits, 3 NSCLC cell lines (A549, H1299, and H460) and 3 HNSCC cell lines (UM-SCC-11B, UM-SCC-22B, and VU-SCC-120) were transfected with siRNAs targeting a variety of G_2–M phase-related genes. The nontargeting siCONTROL#2 and the PLK1 SMARTpool were used as negative and positive control, respectively. All cell cultures were transfected with 25 nmol siRNA and DharmaFECT1. NSCLC cell line SW1573 was transfected with 0.015 μL DharmaFECT1, cell lines A549 and H1299 with 0.03 μL and 0.025 μL, respectively. HNSCC cell line UM-SCC-11B was transfected with 0.065 μL DharmaFECT1, UM-SCC-22B and VU-SCC-120 with 0.15 μL and 0.03 μL, respectively. Cell viability was measured 96 hours after transfection using CellTiter-Blue reagent (Promega) as described above.

Quantitative RT-PCR

Total RNA was isolated using the RNeasy micro kit (Qiagen) and the quality was controlled by OD 260/280 nm analysis on a Nanodrop (Thermo Fisher Scientific). Complementary DNA was synthesized from 50 ng of RNA template using a high capacity cDNA reverse transcription kit (Applied Biosystems). Amplification of the cDNA was conducted on the ABI/Prism 7500 Sequence Detector System (Taqman-PCR, Applied Biosystems) with universal PCR master mix (Applied Biosystems) and gene-specific expression assays for *KIF11* (Hs00189698_mL), *AURKA* (Hs01582073_mL), and *AURKB* (Hs01582073_mL). For each sample, the cycle number at which the amount of amplified target crossed a predetermined threshold (the C_t value) was determined. To correct for differences in RNA input, β-glucuronidase (*GUSB*; Hs99999908_mL; ref. 17) was used as a reference gene for each RNA sample. The mRNA expression was calculated relative to *GUSB* (ΔC_t method).

Western blot analysis

Western blot analyses were carried out according to standard procedures. Antibodies used for detection are mouse anti-KIF11 (1/1,000 4H3-1F12; Cell Signaling Technology) and mouse anti-β-actin (1/20,000, clone AC-15; Sigma-Aldrich). Proteins were visualized using secondary fluorescently labeled antibodies (1/5,000 goat-anti-mouse-IRDye 680 RD; LI-COR Biosciences). Blots were scanned on the Odyssey infrared imaging system (LI-COR Biosciences). Quantification of the protein level was done using Image J software (NIH) and the protein levels were standardized to β-actin levels.

Cell-cycle analysis

Cells were treated with 4 nmol/L ispinesib (Selleck Chemicals) during 24 hours, after which the cells were incubated with 4 nmol/L 5-bromo-2′-deoxyuridine (BrdUrd; Sigma-Aldrich) for 45 minutes. Cells were subsequently harvested and fixed overnight in 70% EtOH. Next, cells were incubated with 0.5 mg/mL RNAse A in PBS at 37°C. After 30 minutes, cells were washed and resuspended in 5 mol/L HCl with 0.5% Triton X-100. The cells were left for 20 minutes at room temperature, after which the solution was neutralized by addition of 0.1 mol/L $Na_2B_4O_7$. The cells were stained for BrdUrd incorporation using mouse anti-BrdUrd antibodies, followed by fluorescein isothiocyanate (FITC)-conjugated rabbit anti-mouse antibodies (Dako) in PBS with 0.5% Tween-20 and 1% BSA. Staining for DNA content was conducted using propidium iodide. The cell-cycle distribution was analyzed with a BD FACSCalibur flow cytometer (BD Biosciences). Cell-cycle analyses were conducted using BD CellQuest software (BD Biosciences).

Staining of mitotic spindles

Cells were grown on an 8-wells Lab-Tek Chamber Slide (Thermo Fisher Scientific) and treated with 4 nmol/L ispinesib (Selleck Chemicals) for 24 hours. The cells were fixed during 1 hour in 4% formaldehyde (Fluka Chemika) and subsequently permeabilized with 0.5% Triton-X100 (ICN Biochemicals). An anti-α-tubulin antibody (clone B-7; Santa Cruz Biotechnology) was applied in a 1:100 dilution for 40 minutes to visualize mitotic spindles. A FITC-labeled anti-mouse antibody (Dako) was used as secondary antibody. The DNA was visualized with 4′,6-diamidino-2-phenylindole dihydrochloride (DAPI; Sigma-Aldrich). The slides were mounted with fluorescence mounting medium (Dako).

Efficacy of ispinesib *in vivo*

Female nu/nu mice were obtained from Harlan Laboratories (Boxmeer). Cell lines VU-SCC-OE and UM-SCC-22A were subcutaneously injected. Resulting xenograft tumors were measured twice a week and treatment started when tumors reached sizes between 100 and 200 mm^3. Mice were treated intraperitoneally with ispinesib (10 mg/kg) or with the ispinesib diluent every 3.5 days during 2 weeks. Again, tumor sizes and body weight were checked twice a week. Mice were sacrificed when one of the tumors reached a volume over 1,000 mm^3 or 90 days after the first ispinesib/diluent injection.

All animal experiments were carried out according to the NIH Principles of Laboratory Animal Care and Dutch national law (Wet op de dierproeven, Stb 1985, 336).

Results

A large panel of genes is involved in cell viability

The NSCLC cell line SW1573 and the HNSCC cell line VU-SCC-120 were subjected to an optimization procedure for automated high-throughput forward siRNA transfection. An siRNA SMARTpool targeting *PLK1*, a gene essential for cancer cell viability (18, 19), was used as positive control. Optimal transfection conditions resulted in a reduction of at least 70% cell viability in the *PLK1* siRNA-transfected cells as compared with siCONTROL#2, a nontargeting siRNA. In addition, more than 80% gene-specific knockdown was observed by quantitative real-time PCR (qRT-PCR; data not shown). Introduction of siCONTROL#2 did not reduce cellular viability with more than 10% to 20% compared with untransfected cells, indicating that the transfection protocols did not lead to excessive nonspecific cell death.

With these optimal transfection conditions, we conducted screens to identify genes that influence cell viability in the NSCLC cell line SW1573 cells and in the HNSCC cell line VU-SCC-120. To identify tumor-lethal siRNAs, both cell lines were seeded in 96-well plates and transfected with the genome-wide siRNA library, containing 21,121 pools of 4 siRNAs, that all target a specific gene. The positive control PLK1 and the negative siCONTROL#2 were loaded on each plate in quadruplicate. The effect of each siRNA on the viability of the cells was analyzed by CellTiter-Blue assay (VU-SCC-120) or automated counting of nuclei (SW1573). Comparison of the 2 independent duplicate screens, showed high reproducibility with a Spearman $\rho = 0.748$ for the duplicate screen in SW1573, and 0.843 for the duplicate screen in VU-SCC-120. Raw viability values were

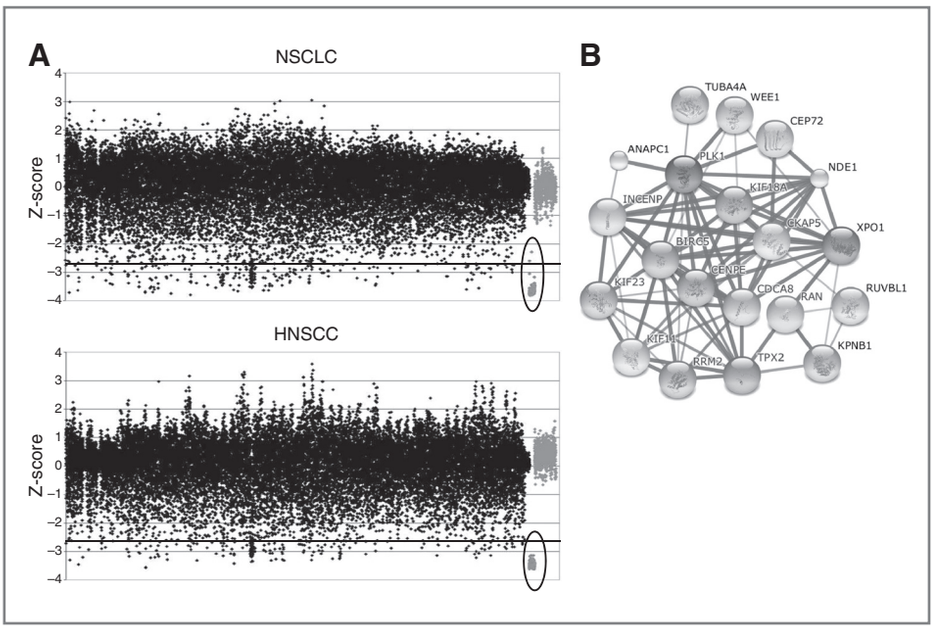

Figure 1. Identification of genes essential for NSCLC and HNSCC tumor cell viability by genome-wide siRNA screens. A, *Z*-score calculations were conducted using cell counts (NSCLC, top) or cell viability measurements (HNSCC, bottom). Black dots represent the *Z*-score for individual siRNA pools that target one gene. *PLK1* siRNAs were used as positive controls and are indicated as gray dots (encircled). Nontargeting siRNAs (siCONTROL) were used as negative controls and are shown in gray. The $Z = -2.75$ threshold (black line) was used to determine siRNAs that significantly influenced tumor cell viability ($P < 0.003$). *Z*-scores were calculated using the mean value per siRNA from the 2 independent siRNA screens. B, a cluster of 20 genes involved in the mitotic spindle checkpoint was identified among the 362 siRNAs that decreased cell viability in NSCLC and/or HNSCC.

normalized per plate and between replicates, and *Z*-scores were calculated. A cutoff of $Z = -2.75$ ($P < 0.003$) yielded 293 siRNAs that significantly decreased cell viability in SW1573 as compared with siCONTROL transfections and 140 siRNAs that caused a lethal phenotype in VU-SCC-120 (Fig. 1A and Supplementary Tables S1 and S2). None of the 1,088 siCONTROL transfections present in the screens reached this threshold, whereas, in total, 99.3% and 100% of the *PLK1* controls were scored as lethal in the NSCLC and HNSCC cell lines, respectively.

To identify common pathways that are essential for tumor cell survival, we subjected the obtained hits to cluster analysis. First, we clustered the 71 genes that were found to be essential for tumor cell survival in both NSCLC and HNSCC using the STRING database (version 9.0), and this revealed 3 clusters that contained genes involved in RNA processing, ribosome biogenesis, and protein modification/ubiquitination (Supplementary Fig. S1A). Because we used a stringent cutoff of $Z = -2.75$, it is likely that we excluded siRNAs that do give a lethal phenotype in only one of the cell lines, whereas it just did not reach the cutoff in the other cell line. Therefore, we also combined the NSCLC and the HNSCC hit lists for cluster analysis. This analysis yielded 362 hits in total, which again contained the same clusters, but with many more genes per cluster (Supplementary Fig. S1B). One cluster consisted of 20 genes involved in the regulation of the G_2–M phase of the cell cycle (Fig. 1B). It is known that in both NSCLC and HNSCC, the cell-cycle checkpoints at G_1 and G_2 are often inactivated by abrogation of the p53 and pRb pathways. The hits identified in the G_2–M phase might consequently relate to these specific aberrations and we therefore analyzed these in more detail.

Mitotic spindle assembly and stabilization is vital

We selected 6 genes from the hits in the G_2–M cluster that are all involved in mitotic spindle organization and stability. For each of these genes, we tested the 4 separate siRNAs that make up the siRNA pools in the genome-wide screens. The phenotype caused by the introduction of these separate siRNAs was retested in the cell lines used in the genome-wide screens and 4 additional NSCLC and HNSCC cell lines (Fig. 2A and Supplementary Fig. S2A–S2E). Inhibition of 4 of the selected genes (*CKAP5*, *KPNB1* (importin-β), *RAN*, and *TPX2*) resulted in more than 50% cell death in all cell lines tested with at least 2 of 4 siRNAs. This shows that expression of these genes is essential in a broad panel of tumor cell lines. We could not validate *CDCA8* as a hit in any of the used cell lines (Supplementary Fig. S2A), indicating that this was likely a false positive hit in VU-SCC-120. The siRNAs targeting *KIF11* mRNA showed a cell killing phenotype in all cell lines, except for SW1573. This was not unexpected, as the *KIF11* siRNA pool was not scored as a hit in the primary genome-wide siRNA screen in this cell line. We confirmed that the siRNA does target the mRNA of *KIF11* in SW1573, as a qRT-PCR showed a *KIF11* mRNA knockdown of more than 94%, whereas the protein level was decreased with more than 82% (Supplementary

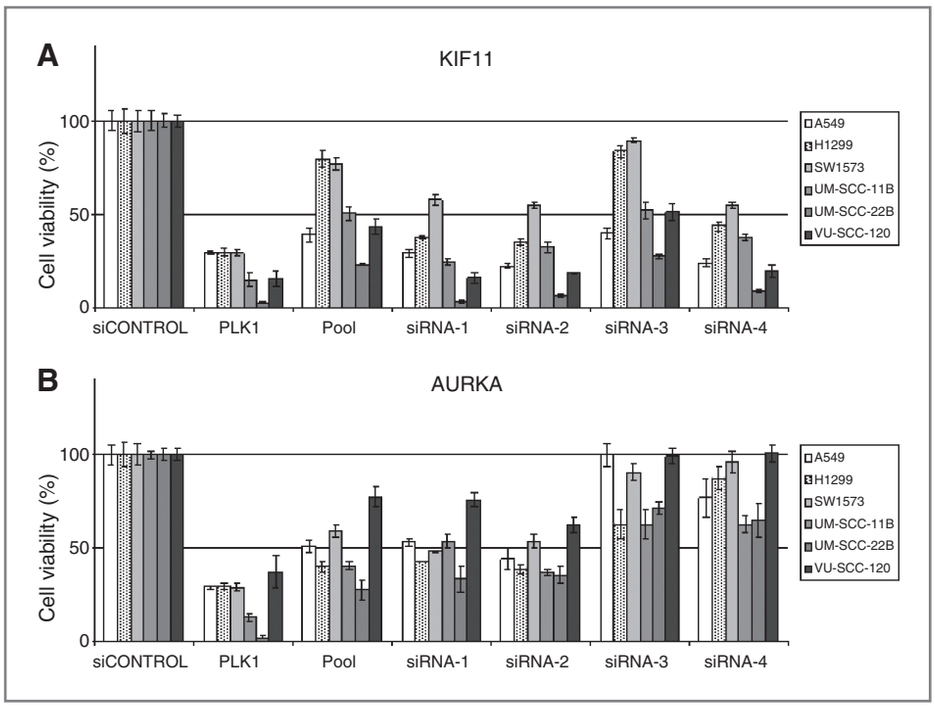

Figure 2. Deconvolution of siRNA pools that decreased NSCLC and HNSCC cell viability. A, three NSCLC (A549, H1299, and SW1573) and 3 HNSCC (VU-SCC-120, UM-SCC-11B, and UM-SCC-22B) cell lines were transfected with the *KIF11* siRNA pool and the 4 individual siRNAs to determine the specificity of the lethal phenotype observed in the genome-wide screens. Cell viability was determined in triplicate and calculated relative to siCONTROL-transfected cells. Bars are median cell viability values and error bars represent the SD. All HNSCC cell lines showed the lethal phenotype with at least 3 out of 4 siRNAs. All NSCLC cell lines showed similar results, except for SW1573. B, the *AURKA* pool and individual siRNAs were deconvoluted but showed a less convincing cell killing phenotype than *KIF11* siRNAs.

Fig. S3A and S3B). Altogether, these data show that 5 of 6 tumor-lethal gene hits involved in the G_2–M phase could be validated in a broad panel of cell lines.

One of the strongest and most consistent hits was *RAN*. However, 3 genes associated with spindle formation via RAN signaling (*DLG7*, *NUTF2*, and *RCC1*) were not identified as putative hits in the genome-wide screens. In subsequent deconvolution experiments, siRNAs targeting these genes indeed confirmed that their role does not seem to be essential for cell survival (Supplementary Fig. S2F–S2H).

Surprisingly, aurora kinases did not seem to be lethal tumor hits in the genome-wide screens, even though *AURKA*, *AURKB*, and *AURKC* have emerged as key mitotic regulators (20–22) and have been explored as promising drug targets (23). We therefore deconvoluted the siRNA pools of the AURK genes and analyzed the cell viability in 3 HNSCC and 3 NSCLC cell lines (Fig. 2B and Supplementary Fig. S4A and S4B). *AURKA* inhibition showed an effect (>50% cell death) on the cell viability of 3 of 6 cell lines tested, whereas *AURKB* and *AURKC* did not show a phenotype in any of the cell lines. We tested the level of knockdown induced by all siRNAs used and concluded that the lack of phenotype is not technical as all siRNAs showed significant mRNA knockdown (Supplementary Fig. S4C and S4D). Next, we explored the possibility that the aurora kinases have a redundant function by simultaneous knockdown of these genes (Supplementary Fig. S4E and S4F). None of the combinations resulted in an increase in cell death. Altogether, many hits identified in the initial screens could be validated, whereas more or less expected hits that were not found were also not confirmed in deconvolution experiments. This observation, although based on limited numbers of genes, shows the accuracy of the obtained hit list of these tumor lethal siRNAs.

Functional *KIF11* is essential for cell viability

We showed that multiple genes that act during the G_2–M phase of the cell cycle are apparently crucial for the viability of NSCLC and HNSCC cells, which makes these genes potential targets for therapy (Fig. 2A). These genes included the microtubule motor protein *KIF11*. Treatment of cell lines with ispinesib (SB-715992), a potent and highly selective small-molecule inhibitor of KIF11 (24), confirmed that functional KIF11 is important for cell viability (Fig. 3). When treated with ispinesib, primary human oral keratinocytes and fibroblasts only showed a mild growth inhibition (approximately 40% compared with untreated controls), whereas cell lines derived from human HNSCCs were completely inhibited in their growth (Fig. 3B). Also, NSCLC cell lines encountered growth inhibition when ispinesib was applied (Fig. 3A), but this effect seemed less dramatic when compared with the HNSCC cell lines. Cell line SW1573 was only marginally affected in its growth after ispinesib incubation, which is in line with the observation that knockdown of *KIF11* expression resulted in only a minor growth inhibiting effect in this cell line.

Next, we checked the basal expression level of *KIF11* in all NSCLC and HNSCC cell lines used and determined that the overall *KIF11* expression was significantly higher in the NSCLC cell lines ($P = 4.44 \times 10^{-6}$; Fig. 3C and Supplementary Fig. S5) than in the HNSCC cell lines. This suggests that the mild phenotype after *KIF11* knockdown or drug inhibition in NSCLC cell lines might be the result of higher

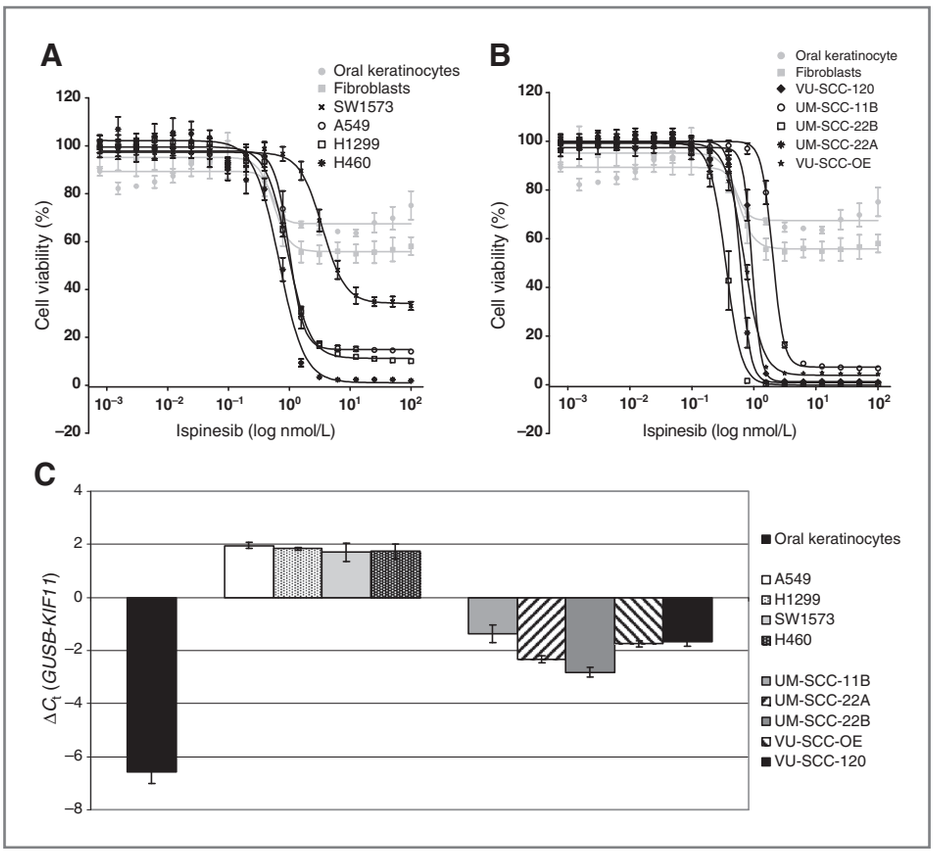

Figure 3. KIF11 is important for NSCLC and particularly HNSCC cell viability. A, four NSCLC cell lines (black lines) were treated with 18 concentrations of ispinesib (SB-715992), a small-molecule inhibitor of KIF11. All cell lines showed growth inhibition after ispinesib treatment, whereas primary oral keratinocytes and fibroblasts (gray lines) only displayed mild effects. SW1573 was the most insensitive cell line among the NSCLC panel. B, five HNSCC cell lines were exposed to 18 concentrations of ispinesib. All 5 cell lines (black lines) showed major growth inhibition. C, the *KIF11* expression level of cultured HNSCC and NSCLC cell lines was determined. Oral keratinocytes (represented by the black bar) showed very low *KIF11* expression as compared with the tumor cell lines. The NSCLC cell lines (A549, H1299, SW1573, and H460) showed higher *KIF11* expression levels than the HNSCC cell lines (VU-SCC-120, UM-SCC-11B, and UM-SCC-22B). This corresponds to the lower sensitivity to ispinesib seen in A and B. Bars represent median values of 3 independent measurements and error bars represent the SD.

KIF11 expression. On the other hand, the expression of *KIF11* in SW1573 does not differ from the other NSCLC cell lines, suggesting that the lack of response to ispinesib treatment is not related to an exceptionally high KIF11 expression in SW1573.

On the basis of the tumor cell killing phenotype after siRNA knockdown as well as ispinesib treatment, we concluded that particularly HNSCC cell lines are tremendously sensitive to KIF11 inhibition and in subsequent experiments we focused on these cell lines. Ispinesib inhibits the interaction between KIF11 and microtubules, thereby blocking the formation of a functional bipolar mitotic spindle, leading to cell-cycle arrest in mitosis and subsequent cell death (24). We investigated the improper mitotic spindle formation in the presence of ispinesib in 2 HNSCC cell lines. Indeed, 100 of 100 dividing tumor cells (100%) treated with ispinesib showed monopolar mitotic spindles (Fig. 4A), whereas 55 of 202 dividing primary keratinocytes (27%) showed monopolar spindles ($P < 0.001$, Fisher exact probability test). In addition, we examined the cell-cycle distribution in HNSCC cell lines in the presence of ispinesib and found accumulation of cells in G_2 phase (Fig. 4B and Supplementary Fig. S6). As expected from the growth inhibition experiments with ispinesib, fibroblasts did not show G_2 arrest to the same degree. This indicates that KIF11 seems a suitable HNSCC drug target with less effect on nontumorigenic cells.

Efficacy of ispinesib in preclinical HNSCC cancer models

Next, we analyzed the efficacy of ispinesib *in vivo*. Mice bearing tumor xenografts of HNSCC cell lines UM-SCC-22A and VU-SCC-OE were treated intraperitoneally with ispinesib (10 mg/kg) at a every 3.5 days during 2 weeks schedule or with the ispinesib diluent. A significant decrease in tumor volume was measured in both xenograft models ($P < 0.001$ for both VU-SCC-OE and UM-SCC-22A at day 14, Student t test), with the longest lasting effect seen in the VU-SCC-OE xenografts (Fig. 5).

Discussion

We used genome-wide loss-of-function screens in a HNSCC and a NSCLC cell line to identify genes influencing cell viability. We identified 362 genes that are essential for cellular survival and this list contained a cluster of genes that coordinately regulate the G_2–M phase transition. We could validate *TPX2*, *CKAP5*, *RAN*, *KPNB1*, and *KIF11* as essential genes for tumor cell survival in HNSCC and NSCLC. In sharp contrast, the aurora kinases (AURK) seemed less important for the survival of both tumor types, although these are also involved in the regulation of the same process. AURKs have previously been reported as promising anticancer targets, and approximately 20 inhibitors targeting these kinases have entered clinical trials (25). Our study, however, suggests that multiple other genes involved in G_2

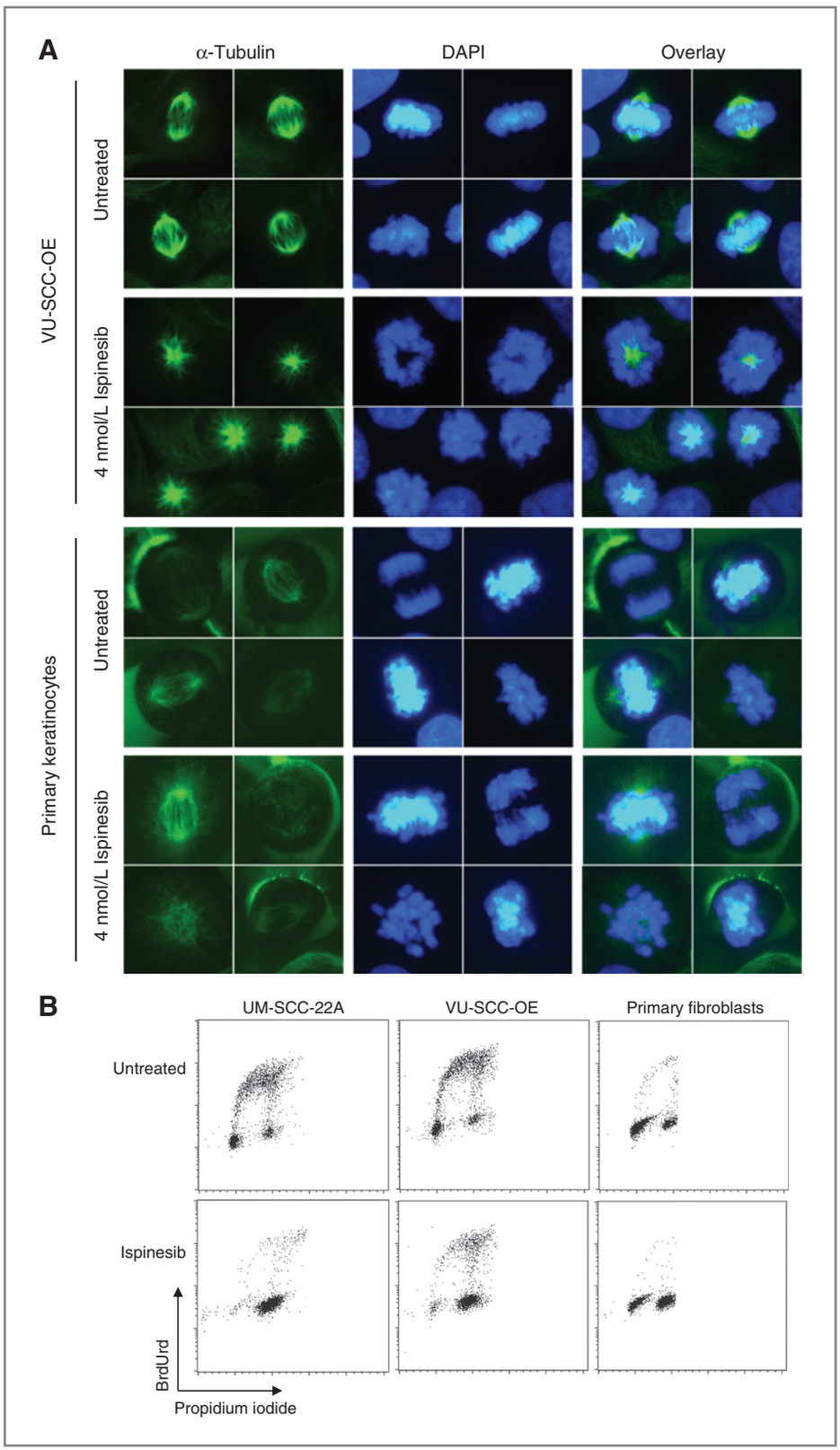

Figure 4. Inhibition of KIF11 impairs mitotic spindle formation and induces G_2 arrest. A, HNSCC cell line VU-SCC-OE showed normal mitotic spindles (top), whereas the bipolar mitotic spindles were replaced by monopolar spindles after incubation with ispinesib (panels at second row). Also, the alignment of the condensed chromosomes at the metaphase plate is abrogated after ispinesib incubation. Pictures were taken using a ×40 magnification. Primary keratinocytes showed normal mitotic spindles (third row) and this was hardly altered after ispinesib treatment (bottom). B, HNSCC cells treated with ispinesib showed accumulation of cells in the G_2–M phase of the cell cycle as compared with untreated cells. In primary fibroblasts, this increase in G_2 accumulation was significantly less compared with the tumor cell lines ($P < 0.001$ for both cancer cell lines, Fisher exact probability test). Measurements were carried out in 2 independent experiments.

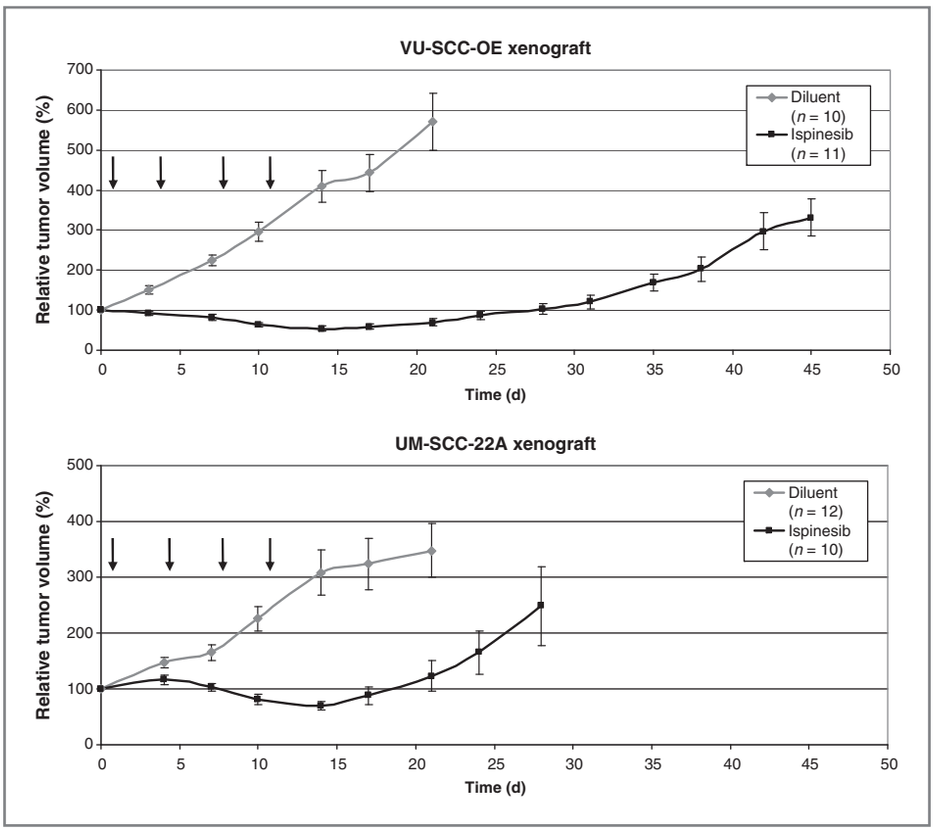

Figure 5. Antitumor activity of ispinesib in HNSCC xenograft models. Ispinesib diluent (gray) and ispinesib (black, 10 mg/kg) were injected according to a q3.5dx4 schedule. Arrows indicate the days of ispinesib administration. The relative tumor volume is depicted as the mean of all tumors within a group and error bars represent the SEM.

–M phase progression might be much more potent targets for therapy particularly in head and neck cancer and perhaps even in lung cancer.

The process of cell-cycle deregulation has attracted great attention as a putative target for intervention. This has lead to the development of U.S. Food and Drug Administration-approved mitotic spindle drugs like taxanes and vinca alkaloids (26, 27). As these drugs have severe toxic side-effects, including neurotoxic effects, there is a need to identify potential new drugs that selectively target proteins that are essential in regulating the G_2–M process. The study presented here can therefore serve as a rich source for the identification of novel putative drug targets.

KIF11 plays a critical role during the establishment of a bipolar mitotic spindle. Failure to set up a bipolar mitotic spindle due to the inhibition of proper KIF11 functioning results in mitotic arrest, eventually leading to cell death. We confirmed that ispinesib, a small-molecule inhibitor of KIF11, has a strong antitumor effect in *in vivo* experiments with HNSCC xenografts, confirming the potency of the identified hit list for identification of new drug targets. Furthermore, we showed that ispinesib does not influence the viability of primary keratinocytes and fibroblasts, indicating the tumor selectivity of this drug. Thus, our findings support the potential of ispinesib as a therapeutic agent for head and neck cancer. Similar results were reported in preclinical models of breast cancer (28) and other xenograft models (29), suggesting that inhibition of *KIF11* might be applicable as therapeutic agent in a wide variety of tumor types.

Ispinesib was the first inhibitor of KIF11 that advanced to clinical trials. Multiple clinical studies on the antitumor activity of ispinesib confirmed the absence of significant neuro- and gastrointestinal toxicities, which makes ispinesib favorable over other mitotic spindle interfering drugs. Several phase I clinical trials (30–32) and at least 4 phase II trials (33–36) on the application of ispinesib in cancer treatment have been described in literature. The studies were conducted with a variety of dose and treatment schedules in multiple tumor types, making a good comparison between the trials difficult. The best antitumor effect was scored as partial response in 3 of 16 patients with advanced breast cancer (37), and all studies reported some cases of stable disease (30–31).

The convincing effect of ispinesib on HNSCC xenografts *in vivo* is promising and by far exceeds the effect of cisplatin (5 mg/kg) and radiation (3 Gy) on these xenografted tumors (data not shown). We could clearly show that repeated exposure of the xenografts to ispinesib is able to sustain inhibition of tumor growth (Fig. 5). However, when treatment was stopped, the tumors slowly regained their proliferative capacity. When we resumed the ispinesib treatment in these xenografts, we again could inhibit tumor growth (data not shown). This shows that continued ispinesib exposure might be of importance for treatment. The conducted clinical trials have been executed with one dose

of ispinesib every 3 weeks, or 3 doses in a 4-week time span (30–32). Therefore, further optimization of dose schedules with this drug should allow a much higher efficacy of the drug in patients with head and neck cancer. It has also been suggested that the lack of tumor response in patients could be due to limited efficacy of the drug in humans, possibly because of its molecular properties (32). As a second-generation KIF11 inhibitor, SB-743921, showed promising preliminary results in clinical trials (38), a combination of this novel drug and an optimized dosing schedule could be more beneficial for treatment outcome.

In conclusion, we identified 362 putative tumor essential genes, of which 5 were validated to induce tumor cell kill upon inhibition. Of these 5 genes, *KIF11* was shown to be a suitable target for drug treatment *in vitro* and *in vivo*. These promising results urge the development of a satisfying treatment schedule for ispinesib, or the use of more effective second-generation drugs, to use this potent drug to its full potential.

Disclosure of Potential Conflicts of Interest

No potential conflicts of interest were disclosed.

Authors' Contributions

Conception and design: S.R. Martens-de Kemp, R. Nagel, R.H. Brakenhoff
Development of methodology: S.R. Martens-de Kemp, R. Nagel, I.H. van der Meulen, V.W. van Beusechem, R.H. Brakenhoff
Acquisition of data (provided animals, acquired and managed patients, provided facilities, etc.): S.R. Martens-de Kemp, R. Nagel, M. Stigter-van Walsum, I.H. van der Meulen, V.W. van Beusechem, B.J.M. Braakhuis
Analysis and interpretation of data (e.g., statistical analysis, biostatistics, computational analysis): S.R. Martens-de Kemp, R. Nagel, B.J.M. Braakhuis, R.H. Brakenhoff
Writing, review, and/or revision of the manuscript: S.R. Martens-de Kemp, R. Nagel, V.W. van Beusechem, B.J.M. Braakhuis, R.H. Brakenhoff
Administrative, technical, or material support (i.e., reporting or organizing data, constructing databases): S.R. Martens-de Kemp, R. Nagel, M. Stigter-van Walsum, I.H. van der Meulen, R.H. Brakenhoff
Study supervision: R.H. Brakenhoff

Grant Support

This study was conducted within the framework of CTMM, the Centre for Translational Molecular Medicine and supported by AIRFORCE project (grant 03O-103).

The costs of publication of this article were defrayed in part by the payment of page charges. This article must therefore be hereby marked *advertisement* in accordance with 18 U.S.C. Section 1734 solely to indicate this fact.

Received August 2, 2012; revised January 10, 2013; accepted January 27, 2013; published OnlineFirst February 26, 2013.

References

1. Kamangar F, Dores GM, Anderson WF. Patterns of cancer incidence, mortality, and prevalence across five continents: defining priorities to reduce cancer disparities in different geographic regions of the world. J Clin Oncol 2006;24:2137–50.
2. Leemans CR, Braakhuis BJ, Brakenhoff RH. The molecular biology of head and neck cancer. Nat Rev Cancer 2011;11:9–22.
3. Muir C, Weiland L. Upper aerodigestive tract cancers. Cancer 1995; 75:147–53.
4. Travis WD, Travis LB, Devesa SS. Lung cancer. Cancer 1995;75: 191–202.
5. Ragin CC, Modugno F, Gollin SM. The epidemiology and risk factors of head and neck cancer: a focus on human papillomavirus. J Dent Res 2007;86:104–14.
6. Jemal A, Siegel R, Ward E, Murray T, Xu J, Smigal C, et al. Cancer statistics, 2006. CA Cancer J Clin 2006;56:106–30.
7. Ciardiello F, Tortora G. EGFR antagonists in cancer treatment. N Engl J Med 2008;358:1160–74.
8. Rouleau M, Patel A, Hendzel MJ, Kaufmann SH, Poirier GG. PARP inhibition: PARP1 and beyond. Nat Rev Cancer 2010;10:293–301.
9. Vultur A, Villanueva J, Herlyn M. BRAF inhibitor unveils its potential against advanced melanoma. Cancer Cell 2010;18:301–2.
10. Hanahan D, Weinberg RA. The hallmarks of cancer. Cell 2000;100: 57–70.
11. Chan DA, Giaccia AJ. Targeting cancer cells by synthetic lethality: autophagy and VHL in cancer therapeutics. Cell Cycle 2008;7: 2987–90.
12. Scholl C, Frohling S, Dunn IF, Schinzel AC, Barbie DA, Kim SY, et al. Synthetic lethal interaction between oncogenic KRAS dependency and STK33 suppression in human cancer cells. Cell 2009;137: 821–34.
13. Weidle UH, Maisel D, Eick D. Synthetic lethality-based targets for discovery of new cancer therapeutics. Cancer Genomics Proteomics 2011;8:159–71.
14. Lin CJ, Grandis JR, Carey TE, Gollin SM, Whiteside TL, Koch WM, et al. Head and neck squamous cell carcinoma cell lines: established models and rationale for selection. Head Neck 2007;29:163–88.
15. Hermsen MA, Joenje H, Arwert F, Welters MJ, Braakhuis BJ, Bagnay M, et al. Centromeric breakage as a major cause of cytogenetic abnormalities in oral squamous cell carcinoma. Genes Chromosomes Cancer 1996;15:1–9.
16. Brenner JC, Graham MP, Kumar B, Saunders LM, Kupfer R, Lyons RH, et al. Genotyping of 73 UM-SCC head and neck squamous cell carcinoma cell lines. Head Neck 2010;32:417–26.
17. Aerts JL, Gonzales MI, Topalian SL. Selection of appropriate control genes to assess expression of tumor antigens using real-time RT-PCR. Biotechniques 2004;36:84–1.
18. Spankuch-Schmitt B, Bereiter-Hahn J, Kaufmann M, Strebhardt K. Effect of RNA silencing of polo-like kinase-1 (PLK1) on apoptosis and spindle formation in human cancer cells. J Natl Cancer Inst 2002;94:1863–77.
19. Liu X, Erikson RL. Polo-like kinase (Plk)1 depletion induces apoptosis in cancer cells. Proc Natl Acad Sci U S A 2003;100:5789–94.
20. Adams RR, Carmena M, Earnshaw WC. Chromosomal passengers and the (aurora) ABCs of mitosis. Trends Cell Biol 2001;11:49–54.
21. Nigg EA. Mitotic kinases as regulators of cell division and its checkpoints. Nat Rev Mol Cell Biol 2001;2:21–32.
22. Carmena M, Earnshaw WC. The cellular geography of aurora kinases. Nat Rev Mol Cell Biol 2003;4:842–54.
23. Keen N, Taylor S. Aurora-kinase inhibitors as anticancer agents. Nat Rev Cancer 2004;4:927–36.
24. Lad L, Luo L, Carson JD, Wood KW, Hartman JJ, Copeland RA, et al. Mechanism of inhibition of human KSP by ispinesib. Biochemistry 2008;47:3576–85.
25. Dar AA, Goff LW, Majid S, Berlin J, El-Rifai W. Aurora kinase inhibitors–rising stars in cancer therapeutics? Mol Cancer Ther 2010;9:268–78.
26. Jordan MA, Wilson L. Microtubules as a target for anticancer drugs. Nat Rev Cancer 2004;4:253–65.
27. Lens SM, Voest EE, Medema RH. Shared and separate functions of polo-like kinases and aurora kinases in cancer. Nat Rev Cancer 2010;10:825–41.
28. Purcell JW, Davis J, Reddy M, Martin S, Samayoa K, Vo H, et al. Activity of the kinesin spindle protein inhibitor ispinesib (SB-715992) in models of breast cancer. Clin Cancer Res 2010;16:566–76.
29. Carol H, Lock R, Houghton PJ, Morton CL, Kolb EA, Gorlick R, et al. Initial testing (stage 1) of the kinesin spindle protein inhibitor ispinesib by the pediatric preclinical testing program. Pediatr Blood Cancer 2009;53:1255–63.
30. Lee RT, Beekman KE, Hussain M, Davis NB, Clark JI, Thomas SP, et al. A University of Chicago consortium phase II trial of SB-715992 in advanced renal cell cancer. Clin Genitourin Cancer 2008;6:21–4.

31. Burris HA III, Jones SF, Williams DD, Kathman SJ, Hodge JP, Pandite L, et al. A phase I study of ispinesib, a kinesin spindle protein inhibitor, administered weekly for three consecutive weeks of a 28-day cycle in patients with solid tumors. Invest New Drugs 2011;29:467–72.
32. Rath O, Kozielski F. Kinesins and cancer. Nat Rev Cancer 2012;12: 527–39.
33. Knox JJ, Gill S, Synold TW, Biagi JJ, Major P, Feld R. A phase II and pharmacokinetic study of SB-715992, in patients with metastatic hepatocellular carcinoma: a study of the National Cancer Institute of Canada Clinical Trials Group (NCIC CTG IND.168). Invest New Drugs 2008;26:265–72.
34. Tang PA, Siu LL, Chen EX, Hotte SJ, Chia S, Schwarz JK, et al. Phase II study of ispinesib in recurrent or metastatic squamous cell carcinoma of the head and neck. Invest New Drugs 2008;26:257–64.
35. Lee CW, Belanger K, Rao SC, Petrella TM, Tozer RG, Wood L, et al. A phase II study of ispinesib (SB-715992) in patients with metastatic or recurrent malignant melanoma: a National Cancer Institute of Canada Clinical Trials Group trial. Invest New Drugs 2008;26:249–55.
36. Souid AK, Dubowy RL, Ingle AM, Conlan MG, Sun J, Blaney SM, et al. A pediatric phase I trial and pharmacokinetic study of ispinesib: a Children's Oncology Group phase I consortium study. Pediatr Blood Cancer 2010;55:1323–8.
37. Gomez HL, Philco M, Pimentel P, Kiyan M, Monsalvo ML, Conlan MG, et al. Phase I dose-escalation and pharmacokinetic study of ispinesib, a kinesin spindle protein inhibitor, administered on days 1 and 15 of a 28-day schedule in patients with no prior treatment for advanced breast cancer. Anticancer Drugs 2011;23:335–41.
38. Holen KD, Belani CP, Wilding G, Ramalingam S, Volkman JL, Ramanathan RK, et al. A first in human study of SB-743921, a kinesin spindle protein inhibitor, to determine pharmacokinetics, biologic effects and establish a recommended phase II dose. Cancer Chemother Pharmacol 2011;67:447–54.